

# The Gd<sup>3+</sup> complex of 1,4,7,10-tetraazacyclododecane-1,4,7,10-tetraacetic acid mono(*p*-isothiocyanatoanilide) conjugated to inulin: a potential stable macromolecular contrast agent for MRI

Luigi Granato<sup>a,b</sup>, Sophie Laurent<sup>a</sup>, Luce Vander Elst<sup>a</sup>, Kristina Djanashvili<sup>c</sup>, Joop A. Peters<sup>c</sup> and Robert N. Muller<sup>a,b\*</sup>

Reaction of DOTA–NCSA [1,4,7,10-tetraazacyclododecane-1,4,7,10-tetraacetic acid mono(*p*-isothiocyanatoanilide)] with O-(aminopropyl)inulin (degree of polymerization 25) provided a chelate that formed a kinetically extremely stable Gd<sup>3+</sup> complex. No transmetalation was observed with Zn<sup>2+</sup>. The conjugate has a relaxivity of 21.7 s<sup>-1</sup> mM<sup>-1</sup> at 20 MHz and 37 °C, and each molecule of the inulin carries on average 35 Gd<sup>3+</sup> ions. The parameters governing the relaxivity of this material and of a low-molecular-weight model compound prepared by conjugation of DOTA–NCSA and propylamine were evaluated by investigation of their water <sup>1</sup>H longitudinal relaxation rate enhancements at different magnetic fields (NMRD) and by studying variable temperature <sup>17</sup>O NMR data. The high relaxivity of the inulin conjugate can be ascribed to the efficient slowing down of the molecular tumbling by this carrier. The rotational correlation time at 37 °C of this material is 1460 ps, whereas that of the model compound is 84 ps. Furthermore, both complexes do not interact significantly with human serum albumin, as shown by their NMRD profiles, and do not undergo transmetalation by zinc ions. The inulin conjugate thus has potential for application as a contrast agent for MRI, particularly as a blood pool agent. Copyright © 2011 John Wiley & Sons, Ltd.

**Keywords:** gadolinium complexes; contrast agents; relaxivity; magnetic resonance imaging; polysaccharides

## 1. INTRODUCTION

The successful introduction of paramagnetic metal complexes as contrast agents (CAs) for magnetic resonance imaging (MRI) and the fast evolution of the MRI technique have given rise to an increasing demand for more effective and specific contrast media. These pharmacological products are used to enhance the contrast between normal and diseased tissue or to indicate blood flow and/or organ function (1,2). The contrast enhancement by Gd<sup>3+</sup> contrast agents is based on changes in the longitudinal (*T*<sub>1</sub>) and transverse (*T*<sub>2</sub>) relaxation times of the water protons, induced by the presence of paramagnetic substances. Gd<sup>3+</sup> complexes of polyaminopolycarboxylates are often used in medical diagnosis as *T*<sub>1</sub> CAs inducing a positive contrast, i.e. a brightening effect on the image. The gadolinium ion is very efficient in enhancing longitudinal relaxation rates *R*<sub>1</sub> (1/*T*<sub>1</sub>) by virtue of its seven unpaired electrons and its relatively long electronic relaxation times. The efficiency of a CA is usually expressed in terms of the relaxivity (*r*<sub>1</sub>), which is the enhancement of the water proton relaxation rate in s<sup>-1</sup> mM<sup>-1</sup> per Gd<sup>3+</sup> ion. According to the well-established Solomon–Bloembergen–Morgan theory and its modifications (3–5), the relaxivity is governed by a set of physico-chemical parameters, which are related to the molecular structure of the Gd<sup>3+</sup> complex and to its dynamics in solution. The parameters directly correlated to the chemical structure are of primary importance

in the ligand design of efficient CAs. They are: the number of water molecules directly coordinated to the Gd<sup>3+</sup> ion (*q*); the residence lifetime of the coordinated water molecules (*τ*<sub>M</sub>); the rotational correlation time representing the molecular tumbling time of the complex (*τ*<sub>R</sub>); interaction of the complex with water molecules in the second sphere (*q*<sub>ss</sub>-hydration number, and *τ*<sub>ss</sub>-residence time), and longitudinal and transversal electronic relaxation times (*τ*<sub>s1</sub>, *τ*<sub>s2</sub>) (1,6).

Since the introduction of the first MRI CA in clinics, Magnevist<sup>®</sup> (Gd–DTPA), several compounds have come into use, such as Gadovist<sup>®</sup> (Gd–BT–DO3A) and ProHance<sup>®</sup> (Gd–HP–DO3A) (7), but

\* Correspondence to: R. N. Muller, Department of General, Organic and Biomedical Chemistry, NMR and Molecular Imaging Laboratory, University of Mons, 19 Avenue Maistriau, 7000 Mons, Belgium.  
E-mail: robert.muller@umons.ac.be

a L. Granato, S. Laurent, L. Vander Elst, R. N. Muller  
Department of General, Organic and Biomedical Chemistry, NMR and Molecular Imaging Laboratory, University of Mons, 19 Avenue Maistriau, 7000 Mons, Belgium

b L. Granato, R. N. Muller  
CMMI - Center for Microscopy and Molecular Imaging, Rue Adrienne Bolland, 8B-6041 Gosselies, Belgium

c K. Djanashvili, J. A. Peters  
Biocatalysis and General Organic Chemistry, Department of Biotechnology, Delft University of Technology, Julianalaan 136, 2628 BL Delft, The Netherlands

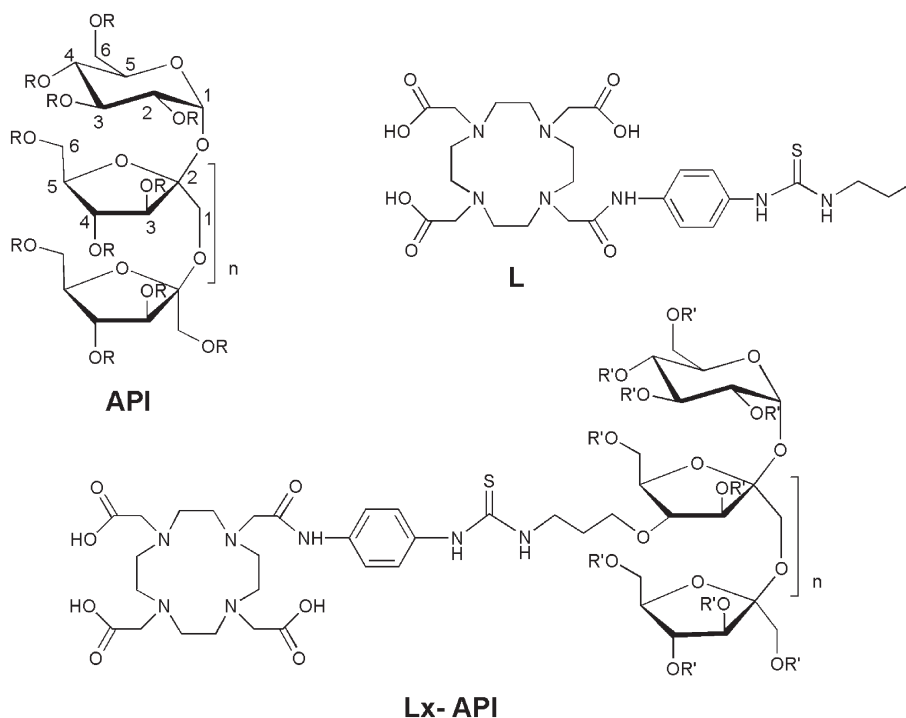
their relaxivities are limited by their small  $\tau_R$  at physiological temperature. The optimal values of  $\tau_R$  are at least 10 ns at 1.5 T (the most common magnetic field used in MRI scanners). To achieve this, these small molecules have been attached via covalent or noncovalent interactions to a number of macromolecules, including albumin (8), carbohydrates (9) and linear polymers such as polylysine (10), dendrimers (11), viral capsids (12) and liposomes (13). The resulting CAs are advantageous because of their increased  $\tau_R$  and their augmented  $Gd^{3+}$  concentration per molecule. Furthermore, the nature of these compounds may serve to prolong their residence time in the cardiovascular system, rendering them amenable to applications in magnetic resonance angiography (MRA). Inulin is one of these compounds. It is a polydisperse polysaccharide consisting of  $\beta(2 \rightarrow 1)$  fructosyl fructose units with one glucopyranose unit at the reducing end. Depending on the source, the degree of polymerization ( $dp$ ) of inulin varies from 10 to 30. This leads to an average molecular weight distribution in a range between 1.5 and 5 kDa, which is favorable for the preparation of macromolecular conjugates (14). Furthermore, inulin and its derivatives possess a low viscosity in aqueous solutions and do not metabolize in blood; both properties can be considered as advantageous for the application of CAs. Previously, we have reported several conjugates of inulin with very favorable relaxivities (15,16). However, the kinetic stabilities of these compounds were lower than that of  $Gd(DTPA)$ , which may preclude applications in view of the recently reported serious adverse side effects upon application of high doses of  $Gd-DTPA$ -bisamides (a complex with relatively low kinetic stability) to patients with severe renal dysfunction.  $Gd-DOTA$  complex and its derivatives are known for their high stability and inertness in physiological medium. Therefore, we report here the synthesis and  $Gd^{3+}$  complexation of the chelate **L** (a DOTA monoamide derivative) and its

conjugate with the modified polysaccharide inulin **Lx-API** (Scheme 1). The relaxivity of both contrast agents and the parameters governing it are evaluated. Also reported and interpreted are Nuclear Magnetic Resonance Dispersion (NMRD) profiles at 37 °C. The relative stability against transmetalation by  $Zn^{2+}$  ions and the possible interaction with human serum albumin (HSA) are evaluated by proton relaxometry. The reported properties of the polysaccharide conjugate demonstrate that they are promising for its application as a CA for MRA.

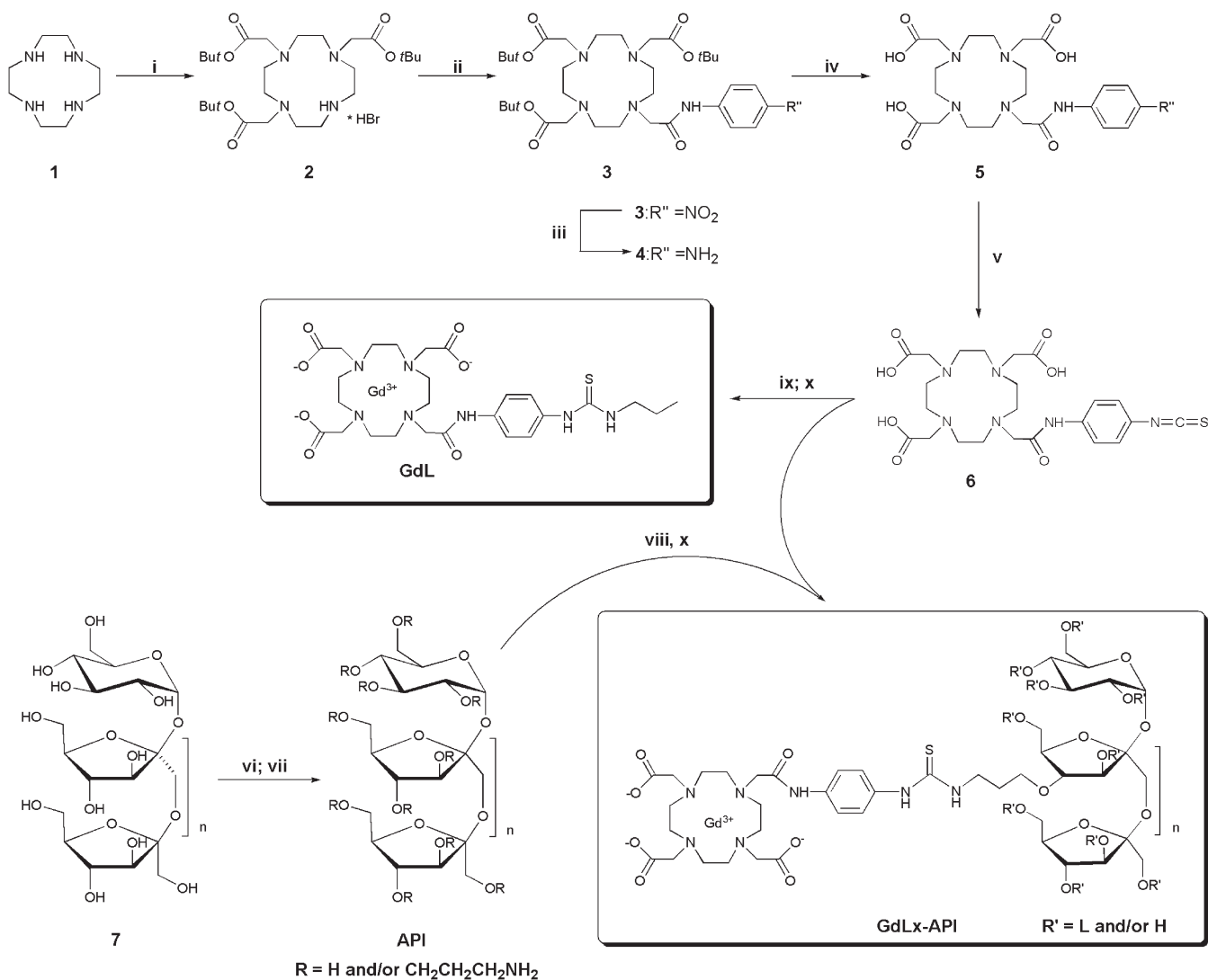
## 2. RESULTS AND DISCUSSION

### 2.1. Synthesis of $Gd^{3+}$ complexes of ligand **L** and its conjugate with API

The chelate (**L**) and its conjugate with inulin (**Lx-API**) were synthesized following the route outlined in Scheme 2. Inulin was chosen because of its high flexibility, which allows the preparation of functionalized derivatives with a high  $ds$  defined as the average number of substituents per monomeric unit of sugar. The theoretical maximum  $ds$  is three, corresponding to the three available hydroxyl groups per sugar unit in the starting material. In the present study, the degree of substitution of *O*-(aminopropyl)inulin (**API**) obtained was 1.4, where the inulin was functionalized by cyanoethylation with acrylonitrile and base, followed by reduction of the cyano groups with metallic Li in liquid ammonia-ethanol at low temperature. Previous studies have indicated that the cyanoethyl groups in *O*-cyanoethylinulin are distributed uniformly along the inulin chain and that, within each fructose unit, the 4-position is the most reactive towards cyanoethylation (17). The ligand **L** was prepared starting from 1,4,7,10-tetrazacyclododecane (**1**). Its protected tri-*tert*-butyl ester (**2**), 1,4,7,10-tetraazacyclododecane-1,4,7-tris



**Scheme 1.** Molecular structures of the conjugates discussed [ $R=H$  and/or  $(CH_2)_3NH_2$ ;  $R'=L$  and/or  $H$ ]. Only one of the three possible positional isomers of **Lx-API** is depicted.



**Scheme 2.** Synthesis of **GdLx-API** and **GdL**: (i) *tert*-butylbromoacetate, NaHCO<sub>3</sub>, CH<sub>3</sub>CN; (ii) 2-chloro-*N*-(4-nitrophenyl)acetamide, K<sub>2</sub>CO<sub>3</sub>, CH<sub>3</sub>CN; (iii) H<sub>2</sub>, Pd/C, EtOH, room temperature; (iv) CF<sub>3</sub>COOH/anisole, CH<sub>2</sub>Cl<sub>2</sub>, room temperature; (v) CCl<sub>4</sub>, CCl<sub>4</sub>/water, room temperature; (vi) acrylonitrile, aqueous NaOH, 45 °C; (vii) Li, liquid NH<sub>3</sub>; EtOH, 50 °C; (viii) water, pH 9–10, room temperature; (ix) water, 1-propylamine, pH 9–10; (x) GdCl<sub>3</sub>·6H<sub>2</sub>O, pH 6.2–6.5.

(acetic acid *t*-butyl ester) (**tDO3AtBu**), was obtained by alkylation using *tert*-butylbromoacetate and base, employing the previously published conditions (18). The 2-chloro-*N*-(4-nitrophenyl)acetamide was attached to **DO3AtBu** by alkylation to give the intermediate **3**. The (*N*-aminophenyl)acetamido **DO3AtBu** derivative **4** was obtained by reduction of the nitro group via hydrogenation with Pd/C (10%) as the catalyst, followed by removal of the *tert*-butyl protective groups by reaction with CF<sub>3</sub>COOH, giving the intermediate **DOTA-AA** (**5**). The amino group of **5** was then converted into the isothiocyanate, which was subsequently used to link **DOTA-NCSA** (**6**) to either propylamine or **API** to give the low-molecular-weight ligand **L** or the macromolecular ligand **Lx-API** (*ds* 1.4), respectively.

## 2.2. Evaluation of the relaxivity and the parameters governing it

In order to determine the efficacy of these Gd<sup>3+</sup> complexes, the longitudinal relaxation rate enhancements of water protons

induced by these complexes were measured as a function of the Larmor frequency. In Fig. 1, the resulting NMRD profiles of **GdLx-API** and **GdL** at 37 °C are compared with that of Gd-DOTA (6,7,19). The shape of the NMRD curve of **GdLx-API**, particularly the local maximum at the resonance frequency of about 20 MHz, is characteristic for high-molecular-weight compounds. It reflects the effect of the relatively long tumbling time of the complex (1,19), whereas the shape of the curve of **GdL** is quite similar to that of Gd-DOTA and is characteristic for low-molecular-weight complexes. The relaxivity of the **GdLx-API** complex is 21.7 s<sup>-1</sup> mM<sup>-1</sup> at 20 MHz and 37 °C, which is quite high considering that clinical MRI exams are performed in a range of magnetic fields between 0.5 and 3 T (20–125 MHz), and that the currently available low-molecular-weight contrast agents have a relaxivity lower than 5 s<sup>-1</sup> mM<sup>-1</sup>. The relaxivity of the present complex is comparable or slightly higher than that of the reported macromolecular conjugates with similar molecular weights (15,16).

The overall relaxivities (*r*<sub>1</sub><sup>obs</sup>) of the Gd<sup>3+</sup> chelates are theoretically described using a model that considers three different

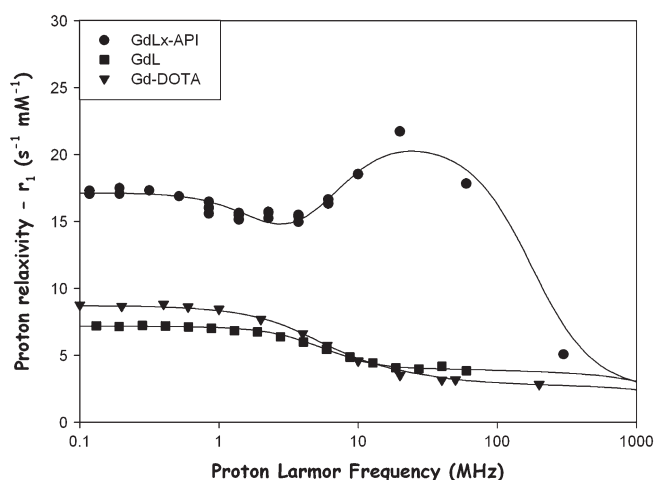


**Figure 1.**  $^1\text{H}$  NMRD profiles of **GdLx-API** 1.18 mM (spheres), **GdL** 2.60 mM (triangles) and **Gd-DOTA** (squares). The lines represent simulations using the best-fit parameters (see Table 1).

contributions: inner sphere ( $r_1^{1S}$ ), outer sphere ( $r_1^{0S}$ ) and second sphere ( $r_1^{2S}$ ) (3,4,20,21). The inner-sphere contribution occurs from the water molecule(s) coordinated directly to the  $\text{Gd}^{3+}$  ion, while the outer-sphere contribution involves all the solvent molecules diffusing along the complex. The term 'second-sphere' concerns contributions arising from water molecules interacting via hydrogen bonds with the electronegative atoms of the ligand, and therefore staying in the second coordination/hydration sphere of  $\text{Gd}^{3+}$  ion. The inner-sphere contribution represents the most important term, and therefore many efforts in the field of MRI CAs are focusing on the optimization of this part.

As described by Solomon–Bloembergen–Morgan equations, the inner-sphere contribution is mainly influenced by the chemical exchange of the water molecule ( $\tau_M$ ), the electron spin relaxation times ( $\tau_{s1}$  and  $\tau_{s2}$ ), the rotational correlation time ( $\tau_R$ ) and the number of water molecules directly coordinated to the  $\text{Gd}^{3+}$  ion ( $q$ ). A previous method for the determination of  $q$  by  $^{17}\text{O}$  chemical shifts (22) used the Dy complexes to perform such measurements, mainly because the contact contribution to its induced shift is predominant as compared with its pseudo-contact shift and because  $\text{Dy}^{3+}$  causes a small broadening of the  $^{17}\text{O}$  signal. However, despite the quite large broadening of the  $^{17}\text{O}$  signal induced by  $\text{Gd}^{3+}$ , this ion is better suited for such measurements since it induces only contact shift and no pseudo-contact shift. With the high-resolution spectrometers now available, it is quite easy to use Gd complexes instead of Dy complexes to perform these measurements. The method uses comparison of the  $^{17}\text{O}$  chemical shift induced by a Gd complex and the well-described Gd complexes, such as Gd–DOTA (Dotarem) and Gd–DTPA (Magnevist), for which  $q = 1$  has been validated, where the  $q$  values determined by  $^{17}\text{O}$  chemical shift analysis on the Gd complex and by the analysis of the luminescence life time of the Eu-complex were identical (23). The value obtained with **GdLx-API** was estimated to be 0.9 and this agrees with the expected value of Gd–DOTA monoamide derivatives (Fig. 2).

The value of  $\tau_M$  was estimated from the analysis of the temperature dependence of the transverse relaxation rate of  $^{17}\text{O}$  resonance of both complexes (Fig. 3). The experimental data were fitted with a theoretical model as described previously (8,24,25). The following best-fit parameters were determined:  $A/\hbar$ , the hyperfine coupling constant between the oxygen nucleus of the

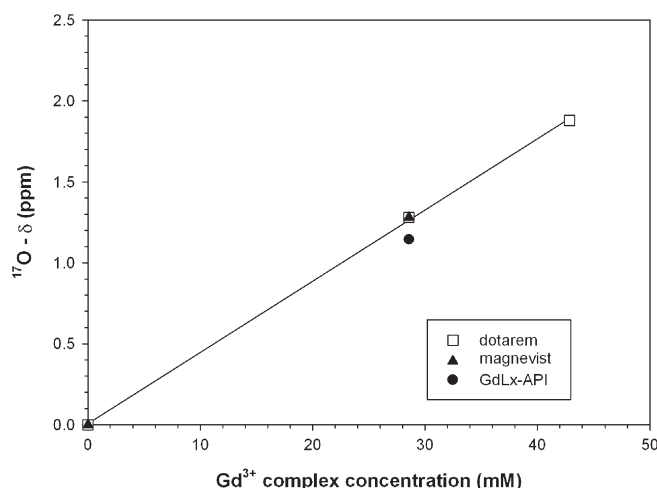


**Figure 2.**  $^{17}\text{O}$  NMR shifts of water versus concentration of  $\text{Gd}^{3+}$  complexes.

bound water molecule and the  $\text{Gd}^{3+}$  ion;  $\tau_v$ , the correlation time modulating the electronic relaxation of  $\text{Gd}^{3+}$ ;  $E_v$ , the activation energy related to  $\tau_v$ ;  $B$ , related to the mean-square of the zero field splitting energy  $\Delta$  ( $B = 2.4\Delta^2$ ); and  $\Delta H^\ddagger$  and  $\Delta S^\ddagger$ , the enthalpy and entropy of activation, respectively, of the water exchange process. The best-fit value of  $\tau_M$  is 625 ns for **GdLx-API** complex and 450 ns for the **GdL** one at 37 °C (Table 1).

It should be noted that the value of  $\tau_M$  is quite high as compared with similar contrast agents reported in the literature. The reason for this difference could be the presence of an amido function that is known to induce an increase of  $\tau_M$  (26). Since  $\tau_M$  limits the relaxivity somewhat, replacement of the chelate by one with a shorter  $\tau_M$  value could give a further increase in the relaxivity.

The temperature dependence of the proton longitudinal relaxivity at constant magnetic field (20 MHz) of **GdLx-API** shows maximum values above 50 °C (Fig. 4), additionally demonstrating the limitation afforded by  $\tau_M$  below 50 °C. This limitation is not observed for **GdL** because of its shorter  $\tau_R$  and thus larger  $T_{1M}$  (relaxation time of the bound water protons) (19).

The  $^1\text{H}$  NMRD profiles of  $\text{Gd}^{3+}$  complexes synthesized were fitted using a model that takes into account inner-sphere, outer-sphere and second-sphere contributions to the paramagnetic relaxation rate. Some parameters were fixed during fitting

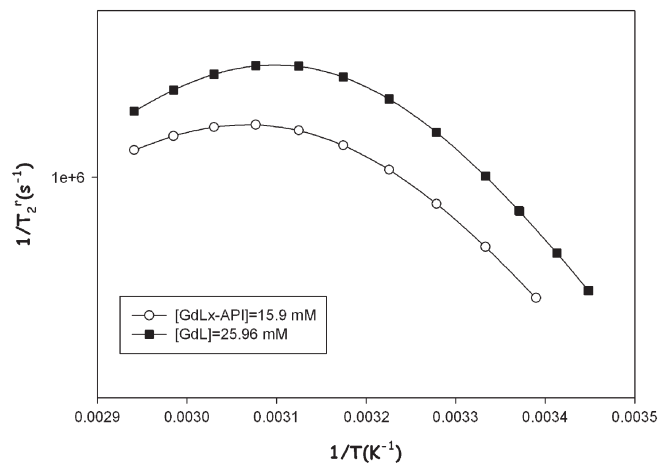


**Figure 3.** Temperature dependence of the reduced  $^{17}\text{O}$  transverse relaxation rate at 11.75 T.

**Table 1.** Parameters for **GdLx-API** and **GdL** obtained from the analysis of  $^{17}\text{O}$  NMR and  $^1\text{H}$  NMRD data compared with **Gd-DOTA (5)**

	<b>GdLx-API</b>	<b>GdL</b>	<b>Gd-DOTA</b>
$\Delta H^\ddagger$ (kJ mol $^{-1}$ )	39.1 ± 0.07	41 ± 0.06	50 ± 0.2
$\Delta S^\ddagger$ (J mol $^{-1}$ K $^{-1}$ )	-0.15 ± 0.23	9.59 ± 0.19	49 ± 0.2
$A/\hbar$ (10 $^6$ rad s $^{-1}$ )	-3.1 ± 0.04	-2.93 ± 0.04	-3.42 ± 0.03
$B$ (10 $^{20}$ s $^{-2}$ )	2.24 ± 0.07	2.93 ± 0.11	1.94 ± 0.09
$E_V$ (kJ mol $^{-1}$ )	20.0 ± 3.19	20.0 ± 16.8	4.0 ± 4.4
$\tau_V^{310}$ (ps)	45 ± 1.0 (6.2) <sup>a</sup>	10.5 ± 1.0 (13) <sup>a</sup>	7 ± 1.0
$\tau_M^{310}$ (ns)	625 ± 34	450 ± 20	122 ± 10
$\tau_R^{310}$ (ps)	1460 ± 70.7	84 ± 3.4	53 ± 1.3
$\tau_{S0}^{310}$ (ps)	153 ± 7.0	92.5 ± 3.2	404 ± 24
$q_{ss}$	5 ± 0.6		
$\tau_{ss}$ (ps)	23.4 ± 1.6		

<sup>a</sup>The first values were obtained from the fitting of the proton NMRD profile; the values in parentheses were obtained from the fitting of the  $^{17}\text{O}$  data.

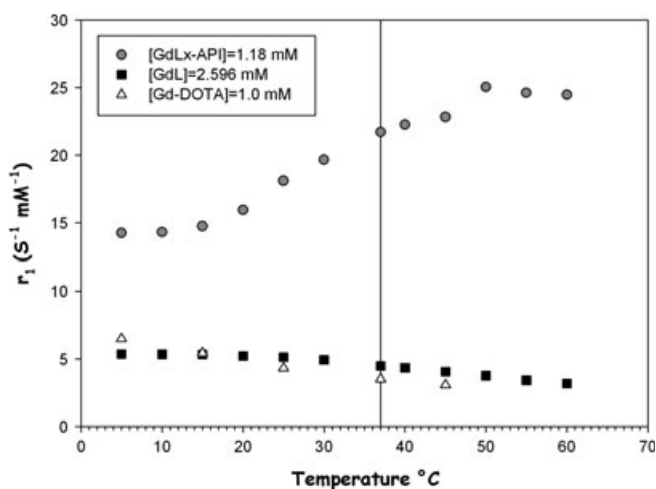
procedure:  $d$ , the distance of closest approach ( $d = 0.4$  nm where a second sphere contribution is present, and  $d = 0.36$  nm in the absence of second sphere contribution);  $D$ , the relative diffusion constant ( $D = 3 \times 10^{-9}$  m $^2$  s $^{-1}$ ); and  $r$ , the distance between the  $\text{Gd}^{3+}$  ion and the proton nuclei of water ( $r = 0.31$  nm). The residence lifetime of the inner sphere,  $\tau_M$ , was set to the value determined by  $^{17}\text{O}$  NMR, the distance between  $\text{Gd}^{3+}$  and the protons of the second sphere water molecules;  $r_{ss}$  was fixed at 0.36 nm. The rotational correlation time ( $\tau_R$ ), the electronic relaxation time at zero field ( $\tau_{S0}$ ) and its correlation time ( $\tau_V$ ), as well as the number of second-sphere water molecules ( $q_{ss}$ ) and the correlation time modulating the second sphere interaction ( $\tau_{ss}$ ), were treated as adjustable parameters. The conjugation of the paramagnetic complex to the inulin carrier resulted in an increase in  $\tau_R$  (1.46 ns) and consequently in a higher relaxivity. In addition, according to the Debye–Stokes–Einstein equation and considering the value of  $\tau_R$  previously calculated for the small complex (**GdL**), the  $\tau_R$  of our macromolecular compound (**GdLx-API**) was estimated to be in the range between 1.5 and 2.9 ns, which is in good agreement with that determined previously (27). In the literature similar inulin systems have been reported such as the  $\text{Gd}^{3+}$  complex of DO3A-squarate and

$\text{H}_5\text{DT4A}^{\text{Ph}}$  chelate linked to aminopropylinulin, which have, respectively,  $\tau_R$  values of 735 and 866 ps (15,16). The divergence between those  $\tau_R$  values and that determined for our complex (**GdLx-API**) is probably due to the molecular structures of different tethers conjugated to the same polymer, which have diverse local mobility owing to different rigidities.

From the fitting of the experimental NMRD profile for **GdLx-API**, we estimated the presence of approximately five second-sphere water molecules. The  $\tau_{ss}$  value obtained from the fitting (23.4 ps) appears to be in good agreement with the values calculated with molecular dynamics for molecules hydrogen-bonded to carboxylates in Gd chelates (28). The high value of  $q_{ss}$  may be ascribed to the presence of a large number of hydroxyl groups on the inulin backbone, which interact with the water molecules coordinated to the Gd chelates and consequently increase their lifetime.

### 2.3. Transmetalation

The  $\text{Gd}^{3+}$  chelates can be sensitive to transmetalation by endogenous ions, such as  $\text{Cu}^{2+}$ ,  $\text{Ca}^{2+}$ , and  $\text{Zn}^{2+}$  (29–33). Out of the three metals mentioned,  $\text{Zn}^{2+}$  combines a rather high concentration (50  $\mu\text{mol l}^{-1}$ ) with a high affinity towards polyaminopoly-carboxylate ligands. Therefore, this metal ion is able to replace a significant amount of  $\text{Gd}^{3+}$ , which may result in release of the toxic  $\text{Gd}^{3+}$  aqua ion in the body (34). To investigate the kinetic stability of the macromolecular complex (**GdLx-API**) and the small complex (**GdL**), we performed a relaxometric study of their transmetalation with  $\text{ZnCl}_2$ . The proton longitudinal relaxation rate of mixtures of  $\text{Gd}^{3+}$  complexes and an equal amount of  $\text{ZnCl}_2$  in phosphate buffer was monitored at 20 MHz and 37 °C. Upon transmetalation of a paramagnetic  $\text{Gd}^{3+}$  ion by a diamagnetic  $\text{Zn}^{2+}$  ion in phosphate buffer, the released  $\text{Gd}^{3+}$  precipitates as  $\text{GdPO}_4$ , which does not contribute to the relaxivity. Therefore, the overall relaxivity of the solution decreases over time with a rate depending on the rate of transmetalation. This decrease in relaxivity is a good estimation of the kinetic stability of the  $\text{Gd}^{3+}$  complexes. The result of this experiment (Fig. 5) shows the very good kinetic stability of both  $\text{Gd}^{3+}$  complexes (**GdLx-API** and **GdL**) as compared with Magnevist, which shows significant decomplexation during the same time period (5 days).


**Figure 4.** Proton longitudinal relaxivity at 20 MHz as a function of temperature.

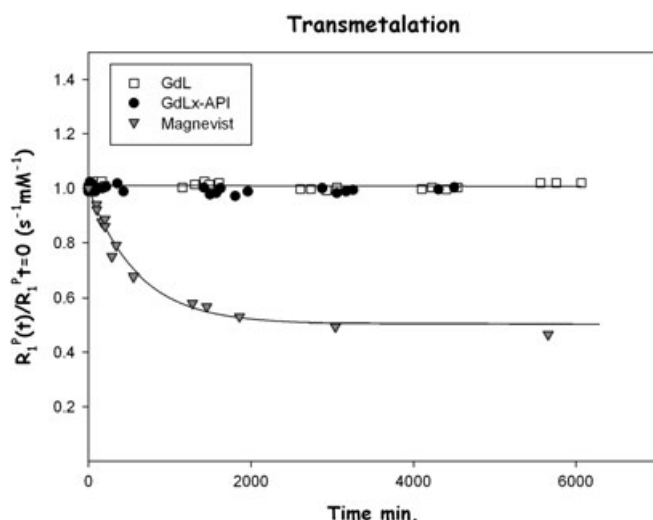


**Figure 5.** Evolution of the water proton paramagnetic longitudinal relaxation rate  $R_1^P(t)/R_1^P(t_0)$  vs time of 2.5 mM  $Zn^{2+}$  aqueous solution for **GdL** (2.5 mM), **GdLx-API** (2.5 mM) and Magnevist (2.5 mM).

#### 2.4. Interaction with HSA

The interaction of low-molecular-weight  $Gd^{3+}$  complexes with HSA increases their rotational correlation time and subsequently enhances their paramagnetic relaxation rates. The resulting increased relaxivity depends on the relative amounts of free and bound CA, and therefore on the strength of the interaction and on the intensity of the magnetic field. When a significant interaction between a low molecular weight Gd complex and HSA takes place, a marked hump around 20 MHz and a clear increase in the low-field paramagnetic relaxation rates are observed (7,25). The proton NMRD profiles of the paramagnetic relaxation rate of solutions containing 1 mM of the contrast agents and 4% of HSA show only a small difference from the curves of their corresponding NMRD profiles in water. For the **GdL** complex, this result agrees with either the absence of interaction with HSA or a negligible interaction (Fig. 6a).

For the **GdLx-API** complex, the small difference between the relaxation rates in the presence and absence of HSA can also be explained by the absence of interaction (Fig. 6b). However, it cannot be excluded that an interaction occurs, but the difference in  $\tau_R$  between bound and free complex is too small to induce a significant  $R_1^P$  increase.

### 3. CONCLUSIONS

We have carried out the synthesis and the measurements of the relaxivity of the  $Gd^{3+}$  of the ligand **L** and its conjugate with oligosaccharide inulin, **GdLx-API**. Analysis of the variable-temperature  $^{17}O$  NMR and  $^1H$  NMRD studies of both complexes confirms that the macromolecular compound **GdLx-API** shows a remarkable increase in relaxivity owing to the decreased local motion. These compounds have a very good kinetic stability at physiological conditions. The relaxivity at 37 °C and 20 MHz is  $21.7 s^{-1} mm^{-1}$ , which corresponds to a relaxivity of  $760 s^{-1}$  per mmol of the molecule. Therefore, upon functionalization of this material with targeting functions, interesting CAs for molecular imaging may be obtained. The high molecular weight may also result in a relatively long residence time in the cardiovascular system, which is interesting for applications in MRA.

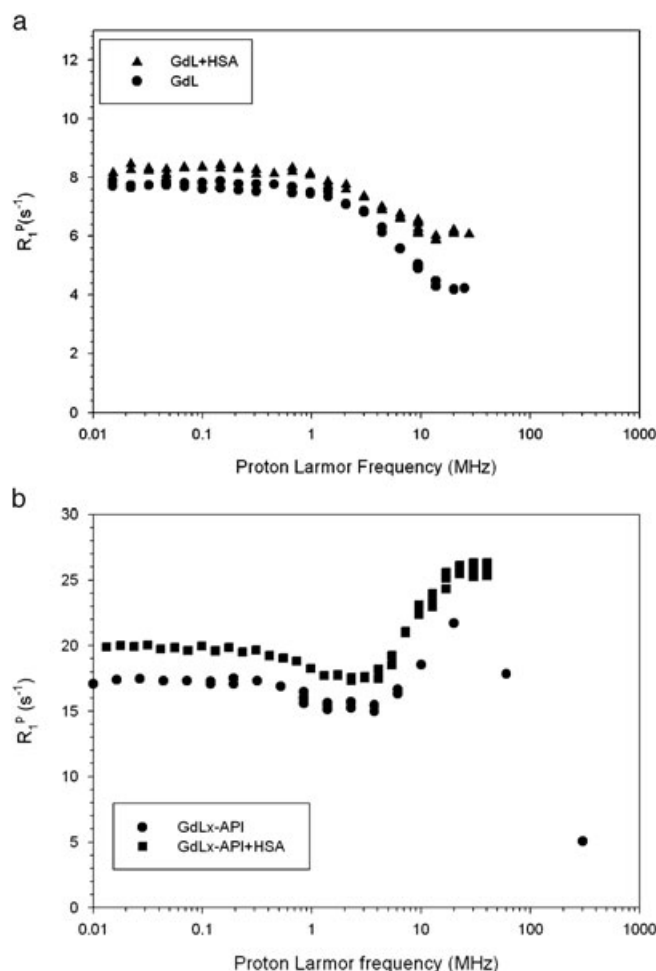


**Figure 6.** Comparison between NMRD profiles of **GdL** (1.0 mM) and **GdLx-API** (1.0 mM), respectively, in the absence and presence of 4% HSA.

## 4. EXPERIMENTAL PROCEDURES

#### 4.1. General methods and materials

All reagent-grade chemicals were purchased from commercial sources and used without further purification. 2-Chloro-*N*-(4-nitrophenyl)acetamide and gadolinium chloride ( $GdCl_3 \cdot 6H_2O$ ) were obtained from Maybridge and Aldrich, respectively. Inulin (*dp* 25) was kindly donated by Sensus Cooperatie Cosun U.A. (Roosendaal, the Netherlands). This 'long-chain' fraction was obtained by recrystallization of inulin from water, thereby selectively removing the low-molecular-weight components. The **API** (Scheme 2), with a degree of substitution (*ds*) of 1.4, was synthesized from inulin (*dp* 25) according to a previously described procedure (35). NMR spectra were recorded on either a Varian Inova-300 or a Bruker Avance II-500 apparatus. Unless stated otherwise, NMR experiments were performed at 25 °C using 5 mm sample tubes. Chemical shifts ( $\delta$ ) are given in ppm. For the measurements in  $D_2O$ , *tert*-butanol was used as an internal standard with the methyl signal referenced to 1.2 ( $^1H$ ) and 31.2 ppm ( $^{13}C$ ). The pH values of the samples were measured at ambient temperature using a Corning 125 pH meter with acalibrated microcombination electrode purchased from Aldrich. The pH values of the solutions were adjusted using dilute aqueous solutions of NaOH and HCl. Mass spectra were

obtained on a Q-TOF Ultima mass spectrometer (Micromass, Manchester, UK). Samples were dissolved in a mixture of H<sub>2</sub>O/MeOH and injected at a rate of 5  $\mu\text{l min}^{-1}$ . The cone voltage was 50 V ( $T=80^\circ\text{C}$ ).

#### 4.2. Synthesis of 1,4,7,10-tetraazacyclododecane-1,4,7-tris(acetic acid *t*-butyl ester) hydrobromide salt (2)

1,4,7,10-Tetraazacyclododecane (5.0 g, 29 mmol) and sodium hydrogen carbonate (8.04 g, 95.7 mmol) were stirred in freshly distilled acetonitrile (160 cm<sup>3</sup>) cooled to 0 °C under N<sub>2</sub>. *Tert*-butyl bromoacetate (18.66 g, 95.7 mmol) was added dropwise over 30 min. After addition, the reaction mixture was allowed to reach ambient temperature and stirred for a further 48 h. The inorganic solids were removed by filtration and the filtrate evaporated under reduced pressure to leave a beige solid. The crude solid product was stirred in toluene for 24 h, offering the title ester (2) as a white solid (11.362 g, 76%). ESI MS:  $m/z$  515 [M + H]<sup>+</sup>,  $m/z$  537 [M + Na]<sup>+</sup>; <sup>1</sup>H NMR (300 MHz, CDCl<sub>3</sub>, 25 °C, TMS):  $\delta$  1.46, 1.47 [27H, s, C(CH<sub>3</sub>)<sub>3</sub>], 2.88–2.94 (12H, m, CH<sub>2</sub>CH<sub>2</sub>), 3.11 (4H, br s, CH<sub>2</sub>CH<sub>2</sub>), 3.30 (2H, s, NCH<sub>2</sub>COO), 3.38 (4H, s, NCH<sub>2</sub>COO), 10.03 (2H, br s, NH<sub>2</sub>). <sup>13</sup>C NMR (300 MHz, CDCl<sub>3</sub>, 25 °C, TMS):  $\delta$  28.21, 28.25, 47.54, 49.22, 51.38, 58.25, 81.71, 81.87, 169.65, 170.54.

#### 4.3. Synthesis of 1,4,7,10-tetraazacyclododecane-1,4,7-tris(acetic acid *t*-butyl ester)-10-acetic acid mono(*p*-nitroanilide) (3)

A suspension of 1,4,7,10-tetraazacyclododecane-1,4,7-tris(acetic acid *t*-butyl ester) hydrobromide (2) (5.654 g, 9.5 mmol) and K<sub>2</sub>CO<sub>3</sub> (1.33 g, 9.5 mmol, 1.0 equiv.) in HPLC-grade CH<sub>3</sub>CN (150 ml) was stirred for 30 min at RT. A 30 ml aliquot of a solution of 2-chloro-*N*-(4-nitrophenyl)acetamide (2.04 g, 9.5 mmol, 1.0 equiv.) in CH<sub>3</sub>CN was added drop-wise to the reaction mixture over 30 min. After 48 h stirring at RT, the mixture was filtered and the solvent evaporated, resulting in an off-white powder (9.12 g). A 2.1 g aliquot of residue product was purified by flash chromatography on silica gel using CH<sub>2</sub>Cl<sub>2</sub>/CH<sub>3</sub>OH (30:1) as mobile phase. After evaporation of the solvent, 1.134 g (1.64 mmol, 55.0 %) of 3 was obtained as a pale-yellow powder. ESI MS:  $m/z$  715 [M + Na]<sup>+</sup>; <sup>1</sup>H NMR (300 MHz, CDCl<sub>3</sub>, 25 °C, TMS):  $\delta$  1.38 [18H, s, C(CH<sub>3</sub>)<sub>3</sub>], 1.44 [9H, s, C(CH<sub>3</sub>)<sub>3</sub>], 1.90–3.70 (24H, m br, CH<sub>2</sub>CH<sub>2</sub>, NCH<sub>2</sub>COO, NCH<sub>2</sub>CON), 4.46–4.56 (2H, m, NHCH<sub>2</sub>Ar), 7.60 (2H, m, ArH), 8.10 (2H, m, ArH), 9.36–9.75 (1H, t, NHCO). <sup>13</sup>C NMR (300 MHz, CDCl<sub>3</sub>, 25 °C, TMS):  $\delta$  27.92, 27.99, 28.13, 42.29, 52.65, 56.16, 81.89, 82.06, 82.13, 123.33, 123.41, 123.70, 128.67, 128.85, 146.65, 147.75, 171.76, 172.30.

#### 4.4. Synthesis of 1,4,7,10-tetraazacyclododecane-1,4,7-tris(acetic acid *t*-butyl ester)-10-acetic acid mono(*p*-aminoanilide) (4)

To a solution of 3.56 g (5.14 mmol) of 1,4,7,10-tetraazacyclododecane-1,4,7-tris(acetic acid *t*-butyl ester)-10-acetic acid mono(*p*-nitroanilide) (3) in 80 ml of EtOH, hydrogenation catalyst (0.9 g of 10% Pd/C) was added. The mixture was stirred for 20 h in an autoclave under H<sub>2</sub> atmosphere (10 bar). The reaction mixture was filtered and the solvent evaporated to yield 2.86 g (84% yield) of the title compound (4) as an off-white powder. ESI MS:  $m/z$  663 [M + H]<sup>+</sup>; <sup>1</sup>H NMR (300 MHz, CDCl<sub>3</sub>, 25 °C, TMS):  $\delta$  1.41 (18H, s, C(CH<sub>3</sub>)<sub>3</sub>), 1.47 (9H, s, C(CH<sub>3</sub>)<sub>3</sub>), 2.65–2.79 (8H, m, CH<sub>2</sub>CH<sub>2</sub>), 2.91 (8H, s, CH<sub>2</sub>CH<sub>2</sub>), 3.17 (6H, s, NCH<sub>2</sub>COO), 3.32 (2H, s, NCH<sub>2</sub>CON), 6.65 (2H, d,  $J=9.3$  Hz, ArH), 7.52 (2H, d,  $J=9.0$  Hz, ArH), 10.32 (1H, br s, NHCO).

<sup>13</sup>C NMR (300 MHz, CDCl<sub>3</sub>, 25 °C, TMS):  $\delta$  28.23, 28.28, 51.71, 52.19, 52.47, 54.70, 55.78, 56.70, 81.01, 115.48, 121.21, 130.57, 142.51, 170.64.

#### 4.5. Synthesis of 1,4,7,10-tetraazacyclododecane-1,4,7,10-tetraacetic acid mono(*p*-aminoanilide) (DOTA-AA) (5)

1,4,7,10-Tetraazacyclododecane-1,4,7-tris(acetic acid *t*-butyl ester)-10-acetic acid mono(*p*-aminoanilide) (4) (2.36 g, 3.56 mmol) was dissolved in CH<sub>2</sub>Cl<sub>2</sub> (5 ml) and CF<sub>3</sub>COOH (1.19 ml, 5 equiv.) and stirred at room temperature for 2 h. Then CF<sub>3</sub>COOH (21 ml) and anisole (21  $\mu\text{l}$ ) were added; the CH<sub>2</sub>Cl<sub>2</sub> was removed by rotary evaporation and the solution was stirred at RT for 48 h. The reaction vessel was cooled to 0 °C and diethyl ether was added. The white precipitate obtained was stirred for 10 min, filtered and then suspended in diethyl ether (this procedure was repeated three times). Then the solvent was evaporated and the resulting solid dried in high vacuum for 4 h to yield 2.83 g of the trifluoroacetic acid salt of the title compound. In order to remove all CF<sub>3</sub>COOH and other impurities, the mixture was eluted through an Amberlite XAD 1600 column following the elution with reverse-phase TLC [MeCN–H<sub>3</sub>PO<sub>4</sub> buffer (1:1) as a mobile phase]. The fractions that contained the product were freeze-dried and 1.54 g (87% yield) of 5 was obtained as a white powder. A purity of 84% was determined by a complexometric titration performed in the presence of the murexide indicator. ESI MS:  $m/z$  495 [M + H]<sup>+</sup>; <sup>1</sup>H NMR (300 MHz, DMSO-*d*<sub>6</sub>, 25 °C, TMS):  $\delta$  3.19 (8H, s, CH<sub>2</sub>CH<sub>2</sub>), 3.31 (8H, s, CH<sub>2</sub>CH<sub>2</sub>), 3.72 (6H, s, NCH<sub>2</sub>COO), 3.97 (2H, s, NCH<sub>2</sub>CON), 6.91 (2H, d,  $J=9.0$  Hz, ArH), 7.46 (2H, d,  $J=8.7$  Hz, ArH), 10.38 (1H, s, NHCO). <sup>13</sup>C NMR (300 MHz, DMSO-*d*<sub>6</sub>, 25 °C, TMS):  $\delta$  49.22, 49.66, 50.14, 50.37, 53.60, 53.87, 55.33 (br s), 119.75, 120.31, 121.24 (br s), 134.20, 134.48 (br s) (CONH), 165.14, 170.67, 171.06 (br s).

#### 4.6. Synthesis of 1,4,7,10-tetraazacyclododecane-1,4,7,10-tetraacetic acid mono(*p*-isothiocyanatoanilide) (DOTA-NCSA) (6)

DOTA-AA (5; 1.54 g, 3.11 mmol) was dissolved in water (10 ml), and the pH was adjusted to 2 by several drops of concentrated aqueous HCl. A solution of thiophosgene (0.375 g, in 5 ml CCl<sub>4</sub>, 3.26 mmol, 1.05 equiv.) was added in one portion, and then the mixture was stirred vigorously at room temperature for 48 h. The excess of thiophosgene was removed by washing the water mixture with CH<sub>2</sub>Cl<sub>2</sub> several times. The water fraction was separated and evaporated to dryness. Yield: 1.56 g. ESI MS:  $m/z$  537 [M + H]<sup>+</sup>; <sup>1</sup>H NMR (300 MHz, DMSO-*d*<sub>6</sub>, 25 °C, TMS):  $\delta$  3.19–3.30 (16H, 2 br s, CH<sub>2</sub>CH<sub>2</sub>), 3.86, 3.98, 4.07 (8H, br s, NCH<sub>2</sub>COO, NCH<sub>2</sub>CON), 7.40 (2H, d,  $J=9.0$  Hz, ArH), 7.62 (3H, br s, COOH), 7.75 (2H, d,  $J=9.0$  Hz, ArH), 11.15, 11.35 (1H, s, NHCO). <sup>13</sup>C NMR (300 MHz, DMSO-*d*<sub>6</sub>, 25 °C, TMS):  $\delta$  49.36 (m), 52.95, 53.30, 54.94, 119.90, 120.15, 123.71, 124.54, 126.38, 132.64, 138.09, 138.19, 165.78, 168.80, 169.30, 170.47.

#### 4.7. Synthesis of 1,4,7,10-tetraazacyclododecane-1,4,7,10-tetraacetic acid mono(*p*-propylthioureidoanilide) (L)

Propylamine (0.093 g, 1.57 mmol) was dissolved in water (5 ml), and the pH was adjusted to 9–10 with diluted NaOH. DOTA-NCSA (6), freshly prepared, 0.848 g (1.58 mmol) was added, and the reaction mixture was stirred at room temperature for 24 h. The crude product (1.078 g) was purified by flash-chromatography (RP-C<sub>18</sub> column) with acetonitrile/H<sub>2</sub>O (8:2) as mobile phase yielding

0.590 g of **L**. ESI MS:  $m/z$  596  $[M + H]^+$ ;  $^1H$  NMR (500 MHz,  $D_2O$ , 25 °C):  $\delta$  0.82 (3H, s,  $CH_3CH_2CH_2$ ), 1.49–1.51 (2H, br m,  $CH_3CH_2CH_2$ ), 3.03–3.41 (10H, br s,  $NCH_2COO$ ,  $NCH_2CON$ ,  $CSNHCH_2CH_2CH_3$ ), 2.35–2.64 (16H, 2 br s,  $NCH_2CH_2N$ ), 7.20 (2H, ArH), 7.47 (2H, ArH).

#### 4.8. Synthesis of API

Inulin (**7**) ( $dp$  25, 5.0 g, 30 mmol of sugar units) was dissolved in 8.9 ml of water (0.49 mmol) containing 0.26 g (6.5 mmol) of NaOH and the mixture was stirred at 45 °C. After addition of 3.28 g (62 mmol) of acrylonitrile the stirring was continued for another hour at 45 °C. The mixture was diluted with water (20 ml) and neutralized by addition of 30% HCl (1 ml), followed by a stepwise addition of small amounts of  $NaHCO_3$  (until  $CO_2$  bubbles were no longer observable). The reaction mixture was evaporated to dryness and the residue was dissolved in 50% ethanol (100 ml). Salts were removed by membrane filtration (20 bar, UTC 60 membrane, Torey Industries Inc., Tokyo, Japan). The product was freeze-dried, yielding 3.956 g of *O*-(cyanoethyl) inulin. The average degree of substitution of 1.53 was determined by integration of the  $^1H$  NMR spectrum, comparing the signals of  $CH_2CN$  (2.7–2.9 ppm) with the signals of remaining protons (3.6–4.5 ppm) (36). *O*-Cyanoethylinulin (500 mg, 2.05 mmol) was dissolved in a mixture of liquid ammonia (50 ml) and dry ethanol (25 ml). Metallic lithium (0.328 g, 47.28 mmol) was added portion-wise during 30 min at –50 °C. The mixture was refluxed for 1 h. Then the ammonia was evaporated over 3 h using a cold water bath, and the resulting mixture was diluted with water (50 ml). A stream of  $CO_2$  was bubbled through the suspension to neutralize LiOH. The mixture was filtered and evaporated to dryness. The product was dissolved in water (100 ml), the salts were removed by membrane ultrafiltration, and the filtrate was freeze-dried to yield 0.286 g of **API**. The degree of substitution was determined by integration of the  $^1H$  NMR spectrum to be 1.4.  $^1H$  NMR ( $D_2O$ , 25 °C, pH 10.5):  $\delta$  1.6–2.0 ( $-O-CH_2CH_2CH_2NH_2$ ), 2.6–3.0 ( $-O-CH_2CH_2CH_2NH_2$ ), 3.5–4.4 (remaining protons).  $^1H$  NMR ( $D_2O$ , 25 °C pH 1.0):  $\delta$  1.7–2.2 ( $-O-CH_2CH_2CH_2NH_2$ ), 2.9–3.2 ( $-O-CH_2CH_2CH_2NH_2$ ), 3.4–4.4 (remaining protons).

#### 4.9. Conjugation of DOTA–NCSA with *O*-aminopropylinulin (**Lx-API**)

*O*-Aminopropylinulin (**API**; 87 mg, 0.40 mmol amino groups) was dissolved in water (5 ml), and the pH was adjusted to 9–10 with diluted NaOH. **DOTA–NCSA** (**6**), freshly prepared, 300 mg (0.56 mmol, 1.4 equiv.) was added and the reaction mixture was stirred at room temperature for 24 h. The reaction mixture was purified by ultrafiltration. The product was freeze-dried, resulting in 0.310 g of **Lx-API** as a white powder.  $^1H$  NMR (300 MHz,  $D_2O$ , 25 °C):  $\delta$  1.8–2.0 ( $CH_2CH_2NH_2$ ), 2.8–3.0 ( $CH_2CH_2NH_2$ ), 3.1–3.3 ( $NCH_2CH_2N$ ), 3.3–3.6 ( $NCH_2COOH$ ), 3.7–4.2 (inulin *H*), 7.43 and 7.54 (4 H, 2 d, ArH). Comparison of the integrals of the aromatic protons and those of the sugar protons indicated that the *ds* was 1.4.

#### 4.10. Preparation of $Gd^{3+}$ complex of **L**

**GdL** was prepared by adding stepwise  $GdCl_3 \cdot 6H_2O$  to a solution of 0.590 g of **L** (0.99 mmol) in 5 ml  $H_2O$ , maintaining the pH between 6.2 and 6.5 by addition of 1 M NaOH. The final pH of the solution after stirring for 48 h was 6.1. The excess of the free lanthanide was removed by centrifugation as  $Gd(OH)_3$  precipitate, which

appeared at pH 9 after addition of 1 M NaOH. The absence of free  $Gd^{3+}$  ions was confirmed by a xylenol orange test (37,38). The pH of the supernatant was decreased to 7 and the solution was freeze-dried, yielding 0.786 g of **GdL** as a white powder. ESI MS:  $m/z$  773  $[M + Na]^+$ .

#### 4.11. Preparation of $Gd^{3+}$ complex of **Lx-API**

**GdLx-API** was prepared by a stepwise addition of  $GdCl_3 \cdot 6H_2O$  to a solution of 0.10 g of **Lx-API** in 4 ml of  $H_2O$ , maintaining the pH between 6.2 and 6.5 by addition of 1 M NaOH. The mixture obtained was stirred for 48 h. Then the product was dialyzed for 24 h with water using a membrane with a cut-off of 1 kDa, until a xylenol orange test showed that no free  $Gd^{3+}$  ions were present in the dialyzate. The final solution of **GdLx-API** was freeze-dried, yielding 0.122 g of a white hygroscopic powder.

#### 4.12. NMRD profiles

$1/T_1$   $^1H$  NMRD profiles were measured on a Stelar Spinmaster FFC fast field cycling NMR relaxometer (Stelar, Mede, Pavia, Italy) over a range of magnetic fields extending from 0.24 mT to 0.7 T and corresponding to  $^1H$  Larmor frequencies from 0.01 to 30 MHz using 0.6 ml samples in 10 mm o.d. tubes. The samples were prepared by dissolution of appropriate amounts of freeze-dried complexes **GdL** and **GdLx-API** in Milli-Q water with the pH in the range 6.2–6.5. The exact  $Gd^{3+}$  concentration was determined by proton relaxivity measurements at 20 MHz and 37 °C after complete hydrolysis in concentrated  $HNO_3$ . Additional relaxation rates at 20 and 60 MHz were obtained with Bruker Minispec mq-20 and mq-60 spectrometers (Bruker, Karlsruhe, Germany), respectively. The 300 MHz data were obtained on a Bruker Avance-300 high resolution spectrometer.

Fitting of the  $^1H$  NMRD was performed with data processing software that uses different theoretical models describing observed nuclear relaxation phenomena (Mint, CERN Library) (39,40). The theoretical model takes into account the inner-sphere interaction (3,4), the outer-sphere interaction (20) and when necessary the second sphere contribution (21).

#### 4.13. $^{17}O$ NMR studies

$^{17}O$  NMR relaxation rate measurements were performed on a Bruker Avance II-500 spectrometer using 5 mm diameter sample tubes containing 325  $\mu$ l (pH 6.2–6.5) of **GdL** (25.96 mM) and **GdLx-API** (15.9 mM) solutions. The temperature was regulated by air or  $N_2$  flow controlled by a BVT-3200 unit.  $^{17}O$  transverse relaxation times of pure water (diamagnetic contribution) were measured using a CPMG sequence and a subsequent two-parameter fit of the data points. The 90 and 180° pulse lengths were 27.5 and 55  $\mu$ s, respectively. Broadband proton decoupling was applied during the acquisition of all  $^{17}O$  NMR spectra.  $^{17}O$   $T_2$  of water in complex solution was obtained from line width measurement. The data are presented as the reduced transverse relaxation rate  $1/T_2^R = 55.55 / ([Gd \text{ complex}] \cdot q \cdot T_2^P)$ , where  $[Gd \text{ complex}]$  is the molar concentration of the complex,  $q$  is the number of coordinated water molecules and  $T_2^P$  is the paramagnetic transverse relaxation rate obtained after subtraction of the diamagnetic contribution from the observed relaxation rate. The treatment of the experimental data was performed as already described (8,24,25).

The number of water molecules in the first coordination sphere ( $q$ ) of the  $Gd^{3+}$  complex (**GdLx-API**) was determined at 60 °C using a Bruker Avance II-500 spectrometer. The tubes with 5 mm external diameter containing 300  $\mu$ l of the sample with 50  $\mu$ l of  $D_2O$  for the lock were used for the measurements. The hydration number  $q$  was obtained by comparing the  $^{17}O$  NMR chemical shifts of **GdLx-API** with those of Gd-DOTA and Gd-DTPA ( $q = 1$ ) (23).

#### 4.14. Transmetalation

The stability of the  $Gd^{3+}$  complexes was determined by a transmetalation method monitoring the  $^1H$  longitudinal relaxation rates of water during 5 days at 37 °C (41). The measurements were performed on a Bruker Minispec mq-20 spin analyzer at 20 MHz using 7 mm sample tubes containing 2.5 mM of  $Gd^{3+}$  complexes and 2.5 mM of  $ZnCl_2$  in 300  $\mu$ l of phosphate buffer solution (26 mM  $KH_2PO_4$ , 41 mM  $Na_2HPO_4$ , pH = 7).

#### 4.15. Interaction with HSA

The interaction of the  $Gd^{3+}$  complexes with HSA was studied by evaluation of the  $^1H$  NMRD profiles of the paramagnetic relaxation rate of the solutions of the complexes (1 mM) under study before and after addition of HSA (4%) (7).

### Acknowledgments

This work was supported by the European Union through a Marie-Curie fellowship (MEST-CT-2004-7442) and the Fonds de la Recherche Scientifique, the ARC Program 05/10-335 of the French Community of Belgium, the ENCITE program of the European Community and the European Regional Development Fund and the Walloon Region (CMMI). The support and sponsorship by COST Action D38 'Metal-based Systems for Molecular Imaging Applications' and the EMIL program are kindly acknowledged. Thanks are due to M. Bia for initial experiments in this project.

### REFERENCES

- Caravan P, Ellison JJ, Mc Murry TJ, Lauffer RB. Gadolinium (III) chelates as MRI contrast agents: structure, dynamics, and application. *Chem Rev* 1999; 99: 2293-2352.
- Merbach AE, Toth E. (eds). *The Chemistry of Contrast Agents in Medical Magnetic Resonance Imaging*. John Wiley & Sons: Chichester, 2001.
- Solomon I. Relaxation processes in a system of two spins. *Phys Rev* 1955; 99: 559-565.
- Bloembergen N. Proton relaxation times in paramagnetic solutions. *J Chem Phys* 1957; 27: 572-573.
- Strandberg E, Westlund P-O.  $^1H$  NMRD profile and ESR lineshape calculation for an isotropic electron spin system with  $S=7/2$ . A generalized modified Solomon-Bloembergen-Morgan theory for non-extreme-narrowing conditions. *J Magn Reson, Ser A* 1996; 122: 179-191.
- Aime S, Botta M, Fasano M, Terreno E. Lanthanide (III) chelates for NMR biomedical applications. *Chem Soc Rev* 1998; 27: 19-29.
- Laurent S, Vander Elst L, Muller RN. Comparative study of the physicochemical properties of six clinical low molecular weight gadolinium contrast agents. *Contrast Med Mol Imag* 2006; 1: 128-137.
- Muller RN, Raduchel B, Laurent S, Platzek J, Pierart C, Mareski P, Vander Elst L. Physicochemical characterization of MS-325, a new gadolinium complex, by multinuclear relaxometry. *Eur J Inorg Chem* 1999; 1949-1955.
- Sirlin C, Vera D, Corbell J, Caballero M, Buxton R, Mattrey R. Gadolinium-DTPA-dextran: a macromolecular MR blood pool contrast agent. *Acad Radiol* 2004; 11: 1361-1369.
- Opsahl L, Uzgiris E, Vera D. Tumor imaging with a macromolecular paramagnetic contrast agent: gadopentetate dimeglumine-polylysine. *Acad Radiol* 1995; 2: 762-767.
- Langereis S, de Lussanet Q, van Engelshoven J, Backes W. Evaluation of Gd(III)DTPA-terminated poly(propyleneimine) dendrimers as contrast agents for MR imaging. *NMR Biomed* 2006; 19: 133-141.
- Anderson EA, Isaacman S, Peabody DS, Wang EY, Canary JW, Kirshenbaum K. Viral nanoparticles donning a paramagnetic coat: Conjugation of MRI contrast agents to the MS2 capsid. *Nano Lett* 2006; 6: 1160-1164.
- Strijkers G, Mulder W, van Heeswijk R, Frederik P, Bomans P, Magusin P, Nicolay K. Relaxivity of liposomal paramagnetic MRI contrast agents. *Magma* 2005; 18: 186-192.
- Stevens CV, Meriggi A, Booten K. Chemical modification of inulin, a valuable renewable resource, and its industrial applications. *Biomacromolecules* 2001; 2: 1-16.
- Lebdušková P, Kotek J, Hermann P, Vander Elst L, Muller RN, Lukeš I, Peters JA. A gadolinium (III) complex of a carboxylic-phosphorus acid derivative of diethylenetriamine covalently bound to inulin, a potential macromolecular MRI contrast agent. *Bioconjug Chem* 2004; 15: 881-889.
- Corsi DM, Vander Elst L, Muller RN, Van Bekkum H, Peters JA. Inulin as a carrier for contrast agent in magnetic resonance imaging. *Chem Eur J* 2001; 7: 64-71.
- Verraest DL, da Silva LP, Peters JA, van Bekkum H. Synthesis of cyanoethyl inulin, aminopropyl inulin and carboxyethyl inulin. *Starch-Stärke* 1996; 48: 191-195.
- Dadabhoy A, Faulkner S, Sammes PG. Long wavelength sensitizers for europium(III) luminescence based on acridone derivatives. *J Chem Soc, Perkin Trans* 2002; 2: 348-357.
- Lauffer RB. Paramagnetic metal complexes as water proton relaxation agents for NMR imaging-theory and design. *Chem Rev* 1987; 87: 901-927.
- Freed JH. Dynamic effects of pair correlation functions on spin relaxation by translational diffusion in liquids. II. Finite jumps and independent T1 processes. *J Chem Phys* 1978; 68: 4034-4037.
- Aime S, Botta M, Fedeli F, Gianolio E, Terreno E, Anelli P. High relaxivity contrast agents for magnetic resonance imaging based on multisite interactions between a  $\beta$ -cyclodextrin oligomer and suitably functionalized  $Gd^{III}$  chelates. *Chem Eur J* 2001; 7: 5262-5269.
- Alpoim CM, Urbano AM, Geraldes CFGC, Peters JA. Determination of the number of inner-sphere water molecules in lanthanide (III) Polyaminocarboxylate complexes. *J Chem Soc Dalton Trans* 1992; 463-467.
- Laurent S, Vander Elst L, Wautier M, Galaup C, Muller RN, Picard C. In vitro characterization of the Gd complex of [2,6-pyridinediylbis(methylene nitrilo)] tetraacetic acid (PMN-tetraacetic acid) and of its Eu analogue, suitable bimodal contrast agents for MRI and optical imaging. *Biorg Med Chem Letters* 2007; 14: 6230-6233.
- Laurent S, Vander Elst L, Houze S, Guerit N, Muller RN. Synthesis and characterization of various benzyl diethylenetriaminepentaacetic acids (dtpa) and their paramagnetic complexes. Potential contrast agents for magnetic resonance imaging. *Helv Chim Acta* 2000; 83: 394-406.
- Vander Elst L, Maton F, Laurent S, Seghi F, Chapelle F, Muller RN. A multinuclear MR study of Gd-EOB-DTPA: comprehensive preclinical characterization of an organ specific MRI contrast agent. *Magn Reson Med* 1997; 38: 604-614.
- Jászberényi Z, Moriggi L, Schimid P, Weidensteiner C, Kneuer R, Merbach AE, Helm L, Tóth E. Physicochemical and MRI characterization of  $Gd^{3+}$ -loaded polyamidoamine and hyperbranched dendrimers. *J Biol Inorg Chem* 2007; 12: 406-420.
- Bertini I, Luchinat C. Relaxation. *Coord Chem Rev* 1996; 150: 77-110.
- Borel A, Helm L, Merbach AE. Molecular dynamics simulations of MRI-relevant  $Gd^{III}$  Chelates: direct access to outer-sphere relaxivity. *Chem Eur J* 2001; 7: 600-610.
- Puttagunta NR, Gibby WA, Puttagunta VL. Comparative transmetalation kinetics and thermodynamic stability of gadolinium-DTPA-bis-glucosamide and other magnetic resonance imaging contrast media. *Invest Radiol* 1996; 31: 619-624.
- Puttagunta NR, Gibby WA, Puttagunta VL. Human in vivo comparative study of zinc and copper transmetalation after administration of magnetic resonance contrast agents. *Invest Radiol* 1996; 31: 739-742.
- Corot C, Idee JM, Hentsch AM, Santus R, Mallet C, Goulas V, Bonnemain B, Meyer D. Structure-activity relationship of macrocyclic and linear gadolinium chelates: investigation of transmetalation

- effect on the zinc dependent metallopeptidase angiotensin-converting enzyme. *J Magn Reson Imag* 1998; 8: 695–702.
32. Corot C, Hentsch AM, Curtelin L. Interaction of gadolinium complexes with metal-dependent biological systems. *Invest Radiol* 1994; 29(suppl. 2): S164–S167.
  33. Cacheris WP, Quay SC, Rocklage SM. The relationship between thermodynamics and the toxicity of gadolinium complexes. *Magn Reson Imag* 1990; 8: 467–481.
  34. Tweedle MF, Hagan JJ, Kumar K, Mantha S, Chang CA. Reaction of gadolinium chelates with endogenously available ions. *Magn Reson Imag* 1991; 9: 409–415.
  35. Verraest DL, Zitha-Bovens E, Peters JA, van Bekkum H. Preparation of O-(aminopropyl)inulin. *Carbohydr Res* 1998; 310: 109–115.
  36. Verraest DL, Peters JA, Kuzee HC, Raaijmakers HWC, van Bekkum H. Distribution of substituents in O-carboxymethyl and O-cyanoethyl ethers on inulin. *Carbohydr Res* 1997; 302: 203–212.
  37. Brunisholz G, Randin M. Sur la séparation des terres rares à l'aide de l'acide éthylènediamine-tétraacétique. IX. Procédé en cycle pour le fractionnement des terres yttrique. *Helv Chim Acta* 1959; 42: 1927–1938.
  38. Corsi DM, Platas-Iglesias C, van Bekkum H, Peters JA. Determination of paramagnetic lanthanide (III) concentrations from bulk magnetic susceptibility shifts in NMR spectra. *Magn Reson Chem* 2001; 39: 723–726.
  39. Vallet P. Relaxivity of nitroxide stable free radicals. Evaluation by field cycling method and optimisation. PhD Thesis, University of Mons, 1992.
  40. Muller RN, Declercq D, Vallet P, Giberto F, Daminet B, Fisher HW, Maton F, Van Haverbeke Y. Proceedings of ESMRMB, 7th Annual Congress, 1990; 394.
  41. Laurent S, Vander Elst L, Copoix F, Muller RN. Stability of MRI paramagnetic contrast media: a proton relaxometric protocol for transmetalation assessment. *Invest Radiol* 2001; 36: 115–122.